Refractive index of humid air in the infrared: model fits

IOP Publishing Journal of Optics A: Pure and Applied Optics
J. Opt. A: Pure Appl. Opt. **9** (2007) 470–476 doi:10.1088/1464-4258/9/5/008

Refractive index of humid air in the infrared: model fits

Richard J Mathar

Leiden Observatory, Leiden University, PO Box 9513, 2300 RA Leiden, The Netherlands

E-mail: mathar@strw.leidenuniv.nl

Received 15 January 2007, accepted for publication 23 March 2007
Published 24 April 2007
Online at stacks.iop.org/JOptA/9/470

Abstract
The theory of summation of electromagnetic line transitions is summarized in terms of the Taylor expansion of the refractive index of humid air as a function of the basic independent parameters (temperature, pressure, humidity, wavelength) in five separate infrared regions from the H to the Q band at a fixed percentage of carbon dioxide. These are least-squares fits to raw, highly resolved spectra for a set of temperatures from 10 to 25 °C, a set of pressures from 500 to 1023 hPa and a set of relative humidities from 5 to 60%. These choices reflect the prospective application to characterize ambient air at mountain altitudes of astronomical telescopes.

Keywords: refractive index, infrared, water vapour, humid air, phase velocity

1. Scope

The literature of optical, chemical and atmospheric physics on the subject of the refractive index of moist air falls into several categories, sorted with respect to decreasing relevance (if relevance is measured by the closeness to experimental data and by the degree of independence to the formalism employed here):

(i) experiments on moist air in the visible [1–4],
(ii) experiments on pure water vapour at 3.4 and 10.6 μm [5–7],
(iii) experiments on dry air and its molecular constituents in the visible [8–11], at 1.064 μm [12, 13], up to 2.0 μm [14], up to 1.7 μm [15–18], or at 10.6 μm [19, 20],
(iv) verification of the dispersion and higher-order derivatives with astronomical interferometry [21],
(v) review formulae [22–26],
(vi) theoretical summation of electronic transitions [27–30].

What follows is in the last category. It provides easy access to predictions of the refractive index of humid air at conditions that are typical in atmospheric physics, in support of astronomical applications [31, 27, 32, 33] and ray tracing [34] until experimental coverage of the infrared wavelengths might render these obsolete. One of the limiting factors of experimental accurate determination of dielectric functions of humid air is the calibration of the actual molecular density in laboratory samples. Ellipsometry of water surfaces faces this problem to a lesser extent; literature on infrared reflectivity is more frequent. Nevertheless, we leave the liquid and solid states of water aside, because density extrapolation of their dielectric response to the gaseous state is difficult by the permanent dipole moment of the molecule.

The approach is in continuation of my earlier work [28] based on a more recent HITRAN database [35] plus more precise accounting of various electromagnetic effects for the dielectric response of dilute gases, to be described in section 2 below. We do not review, paraphrase or duplicate the contents of [28] which demonstrated that a basic linear dielectric response theory can predict refractive indices of gases if supported by a sufficiently broad database of oscillator strengths and locations of atomic and molecular line transitions. The relative accuracy of susceptibilities derived from this line summation is estimated at 2×10^{-4} in section 4. The value of this work is to deliver this in an easily accessible format which renders equivalent programming efforts superfluous to all readers who are neither interested in the underlying quantum chemistry nor in spectroscopic details.

2. Dielectric model of the raw data

The complex valued dielectric function $n(\omega)$ of air

$$n = \sqrt{1 + \bar{\chi}} \tag{1}$$

is constructed from molecular dynamical polarizabilities with the textbook formula

$$\chi_{\mathrm{m}}(\omega) = 2N_{\mathrm{m}}c^2 \sum_l \frac{S_{\mathrm{m}l}}{\omega_{0\mathrm{m}l}} \left(\frac{1}{\omega + \omega_{0\mathrm{m}l} - \mathrm{i}\Gamma_{\mathrm{m}l}/2} - \frac{1}{\omega - \omega_{0\mathrm{m}l} - \mathrm{i}\Gamma_{\mathrm{m}l}/2} \right). \quad (2)$$

N_{m} are molecular number densities, $S_{\mathrm{m}l}$ are the line intensities for the transitions enumerated by l. $\omega_{0\mathrm{m}l}$ are the transition angular frequencies, $\Gamma_{\mathrm{m}l}$ the full line widths at half-maximum. c is the velocity of light in vacuum and i the imaginary unit. The line shape (2) adheres to the complex-conjugate symmetry $\chi_{\mathrm{m}}(\omega) = \chi_{\mathrm{m}}^*(-\omega)$, as required for functions which are real-valued in the time domain. The poles $\pm\omega_{0\mathrm{m}l} + \mathrm{i}\Gamma_{\mathrm{m}l}/2$ in the complex ω-plane are all in the same (upper or lower) half-plane, as for any retarded (causal) response function. The sign convention of $\Gamma_{\mathrm{m}l}$ merely reflects a sign choice in the Fourier transforms and carries no real significance; a sign in the Kramers–Kronig formulae is bound to it. The integrated imaginary part is [36]

$$\int_0^\infty \mathrm{Im}\,\chi_{\mathrm{m}}(\sigma)\,\mathrm{d}\sigma = N_{\mathrm{m}}c \sum_l \frac{S_{\mathrm{m}l}}{\omega_{0\mathrm{m}l}}, \quad (3)$$

where $\sigma = \omega/(2\pi c) = 1/\lambda$ is the vacuum wavenumber.

Line strengths $S_{\mathrm{m}l}$ and positions $\omega_{0\mathrm{m}l}$ are based on the HITRAN list [35, 37, 38] and other sources as described earlier [28]. The results of section 3 include summation over the oscillator strengths of the air components N_2, O_2, Ar, Ne, CO_2, H_2O, O_3, CH_4 and CO. The remaining paragraphs describe some refinements of the computer program relative to its status three years ago [28]. No aspect of the theory or the ansatz is new or even interesting. The achievable quality depends on utilizing spectroscopic databases ($\omega_{0\mathrm{m}l}$, $S_{\mathrm{m}l}$) of all molecular species to the shortest wavelengths available, and to transform the hydrodynamic variables, temperature and pressure, into densities N_{m} with accurate equations of state.

More molecules are packed into a given volume at a given partial pressure than the ideal gas equation predicts. The second virial coefficients for nitrogen and oxygen are negative at typical environmental temperatures, $\approx -7.5 \times 10^{-6}$ m^3 mol^{-1} for nitrogen and $\approx -1.9 \times 10^{-5}$ m^3 mol^{-1} for oxygen at 12 °C [39, 40]. The gas densities of nitrogen and oxygen are $\approx$25 mol m^{-3} and $\approx$6 mol m^{-3} for nitrogen and oxygen, respectively, at air pressures of the order 740 hPa, so the correction factors for the density and for the refractivity are of the order 2×10^{-4} due to this effect, the product of the virial and the density. See [41] for a review and [42] for examples of the cross-talk to refractivities.

The second and third virials for water vapour are larger [43–45]—the second $\approx -1.3 \times 10^{-3}$ m^3 mol^{-1} [46, figure 7.19]—and often placed as 'enhancement factors'. See [47] for a review on this subject and [48] for recent values of the second virial coefficient. The values presented here use the equation of state in a self-consistent solution of the first line of [46, table 6.3] for water, the values of [39, p 239] for nitrogen and the NIST values [49] for the second and third virials of oxygen, argon and carbon dioxide.

The temperature dependence of the partition sums leads to temperature-dependent line strengths [50]. For the HITRAN lines, this has been implemented on a line-per-line basis [51, 52]. The combined change induced by the upgrade to the database of August 2006 plus this increase of the line strengths at lower temperatures is minuscule, less than 2×10^{-9} in the $c_{0\mathrm{ref}}$ coefficients and less than 3×10^{-5} K in the c_{0T} coefficients reported in section 3.

The line broadening parameters Γ were not changed [53, 54] from the ones at the HITRAN reference pressure of 1 atm, since the effect on the real part of the susceptibility is presumably negligible. Effects of molecular clustering [55] have not been considered.

The paramagnetic susceptibility of oxygen and the diamagnetic contribution of nitrogen [56] account for most of the remaining gap between theory and experiment. The volume susceptibility of dry air is $\approx 3.7 \times 10^{-7}$ at 1013 hPa, to increase n by $\approx 1.3 \times 10^{-7}$ [57]. The magnetic dipole transitions of oxygen [58, 59] are incorporated in the HITRAN list [60], which allows us to add dispersion to their response. (Since we are only dealing with the limit of small susceptibilities, the electric and magnetic susceptibilities are additive, which means cross-product terms have been neglected here.) The magnetism of water is negligible because the magnetic moment of the water molecule is close to the magnetic moment of the nitrogen molecule [57, 61], but the abundance of the water molecules in air is much smaller than the abundance of nitrogen molecules.

We incorporate the mutual inter-molecular cross-polarization with the Clausius–Mossotti (Lorentz–Lorenz) formula [62, 63]: the macroscopic susceptibility $\bar{\chi} = n^2 - 1$ inserted in (1) is

$$\bar{\chi} = \frac{\sum \chi_{\mathrm{m}}}{1 - \sum \chi_{\mathrm{m}}/3}, \quad (4)$$

where $\sum \chi_{\mathrm{m}}$ is the sum over all atomic/molecular polarizabilities taken from (2). This increases the real part of χ by $\approx (\sum \chi_{\mathrm{m}})^2/3$, hence the real part of n by $\approx (\sum \chi_{\mathrm{m}})^2/6$, which is of the order 2×10^{-8} if we take $\sum_{\mathrm{m}} \chi \approx 4 \times 10^{-4}$ as a guideline.

3. Fitting results

The least squares fit to the raw data looks as follows:

$$n - 1 = \sum_{j=0,1,2,\ldots} c_j(T, p, H)\,(\sigma - \sigma_{\mathrm{ref}})^j\,; \quad (5)$$

$$\begin{aligned} c_j(T, p, H) = {} & c_{j\mathrm{ref}} + c_{jT}\left(\frac{1}{T} - \frac{1}{T_{\mathrm{ref}}}\right) + c_{jTT}\left(\frac{1}{T} - \frac{1}{T_{\mathrm{ref}}}\right)^2 \\ & + c_{jH}\,(H - H_{\mathrm{ref}}) + c_{jHH}\,(H - H_{\mathrm{ref}})^2 \\ & + c_{jp}\,(p - p_{\mathrm{ref}}) + c_{jpp}\,(p - p_{\mathrm{ref}})^2 \\ & + c_{jTH}\left(\frac{1}{T} - \frac{1}{T_{\mathrm{ref}}}\right)(H - H_{\mathrm{ref}}) \\ & + c_{jTp}\left(\frac{1}{T} - \frac{1}{T_{\mathrm{ref}}}\right)(p - p_{\mathrm{ref}}) \\ & + c_{jHp}\,(H - H_{\mathrm{ref}})\,(p - p_{\mathrm{ref}})\,. \end{aligned} \quad (6)$$

Here, T is the absolute temperature with a reference value of $T_{\mathrm{ref}} = (273.15 + 17.5)$ K, p is the air pressure with a reference value set at $p_{\mathrm{ref}} = 75\,000$ Pa, H the relative humidity

Table 1. Fitting coefficients for the multivariate Taylor expansion (6) to the real part of the index of refraction over the $1.3 \leqslant 1/\sigma \leqslant 2.5$ μm range with $\sigma_{\rm ref} = 10^4/2.25$ cm^{-1}.

j	$c_{j\rm ref}$ (cm^j)	c_{jT} (cm^j K)	c_{jTT} (cm^j K^2)	c_{jH} (cm^j %$^{-1}$)	c_{jHH} (cm^j %$^{-2}$)
0	$0.200\,192 \times 10^{-3}$	$0.588\,625 \times 10^{-1}$	$-3.015\,13$	$-0.103\,945 \times 10^{-7}$	$0.573\,256 \times 10^{-12}$
1	$0.113\,474 \times 10^{-9}$	$-0.385\,766 \times 10^{-7}$	$0.406\,167 \times 10^{-3}$	$0.136\,858 \times 10^{-11}$	$0.186\,367 \times 10^{-16}$
2	$-0.424\,595 \times 10^{-14}$	$0.888\,019 \times 10^{-10}$	$-0.514\,544 \times 10^{-6}$	$-0.171\,039 \times 10^{-14}$	$-0.228\,150 \times 10^{-19}$
3	$0.100\,957 \times 10^{-16}$	$-0.567\,650 \times 10^{-13}$	$0.343\,161 \times 10^{-9}$	$0.112\,908 \times 10^{-17}$	$0.150\,947 \times 10^{-22}$
4	$-0.293\,315 \times 10^{-20}$	$0.166\,615 \times 10^{-16}$	$-0.101\,189 \times 10^{-12}$	$-0.329\,925 \times 10^{-21}$	$-0.441\,214 \times 10^{-26}$
5	$0.307\,228 \times 10^{-24}$	$-0.174\,845 \times 10^{-20}$	$0.106\,749 \times 10^{-16}$	$0.344\,747 \times 10^{-25}$	$0.461\,209 \times 10^{-30}$
j	c_{jp} (cm^j Pa^{-1})	c_{jpp} (cm^j Pa^{-2})	c_{jTH} (cm^j K %$^{-1}$)	c_{jTp} (cm^j KPa^{-1})	c_{jHp} (cm^j %$^{-1}$ Pa^{-1})
0	$0.267\,085 \times 10^{-8}$	$0.609\,186 \times 10^{-17}$	$0.497\,859 \times 10^{-4}$	$0.779\,176 \times 10^{-6}$	$-0.206\,567 \times 10^{-15}$
1	$0.135\,941 \times 10^{-14}$	$0.519\,024 \times 10^{-23}$	$-0.661\,752 \times 10^{-8}$	$0.396\,499 \times 10^{-12}$	$0.106\,141 \times 10^{-20}$
2	$0.135\,295 \times 10^{-18}$	$-0.419\,477 \times 10^{-27}$	$0.832\,034 \times 10^{-11}$	$0.395\,114 \times 10^{-16}$	$-0.149\,982 \times 10^{-23}$
3	$0.818\,218 \times 10^{-23}$	$0.434\,120 \times 10^{-30}$	$-0.551\,793 \times 10^{-14}$	$0.233\,587 \times 10^{-20}$	$0.984\,046 \times 10^{-27}$
4	$-0.222\,957 \times 10^{-26}$	$-0.122\,445 \times 10^{-33}$	$0.161\,899 \times 10^{-17}$	$-0.636\,441 \times 10^{-24}$	$-0.288\,266 \times 10^{-30}$
5	$0.249\,964 \times 10^{-30}$	$0.134\,816 \times 10^{-37}$	$-0.169\,901 \times 10^{-21}$	$0.716\,868 \times 10^{-28}$	$0.299\,105 \times 10^{-34}$

Table 2. Fitting coefficients for the multivariate Taylor expansion (6) to the real part of the index of refraction over the $2.8 \leqslant 1/\sigma \leqslant 4.2$ μm range with $\sigma_{\rm ref} = 10^4/3.4$ cm^{-1}.

j	$c_{j\rm ref}$ (cm^j)	c_{jT} (cm^j K)	c_{jTT} (cm^j K^2)	c_{jH} (cm^j %$^{-1}$)	c_{jHH} (cm^j %$^{-2}$)
0	$0.200\,049 \times 10^{-3}$	$0.588\,432 \times 10^{-1}$	$-3.135\,79$	$-0.108\,142 \times 10^{-7}$	$0.586\,812 \times 10^{-12}$
1	$0.145\,221 \times 10^{-9}$	$-0.825\,182 \times 10^{-7}$	$0.694\,124 \times 10^{-3}$	$0.230\,102 \times 10^{-11}$	$0.312\,198 \times 10^{-16}$
2	$0.250\,951 \times 10^{-12}$	$0.137\,982 \times 10^{-9}$	$-0.500\,604 \times 10^{-6}$	$-0.154\,652 \times 10^{-14}$	$-0.197\,792 \times 10^{-19}$
3	$-0.745\,834 \times 10^{-15}$	$0.352\,420 \times 10^{-13}$	$-0.116\,668 \times 10^{-8}$	$-0.323\,014 \times 10^{-17}$	$-0.461\,945 \times 10^{-22}$
4	$-0.161\,432 \times 10^{-17}$	$-0.730\,651 \times 10^{-15}$	$0.209\,644 \times 10^{-11}$	$0.630\,616 \times 10^{-20}$	$0.788\,398 \times 10^{-25}$
5	$0.352\,780 \times 10^{-20}$	$-0.167\,911 \times 10^{-18}$	$0.591\,037 \times 10^{-14}$	$0.173\,880 \times 10^{-22}$	$0.245\,580 \times 10^{-27}$
j	c_{jp} (cm^j Pa^{-1})	c_{jpp} (cm^j Pa^{-2})	c_{jTH} (cm^{j}K %$^{-1}$)	c_{jTp} (cm^{j}K Pa^{-1})	c_{jHp} (cm^j %$^{-1}$ Pa^{-1})
0	$0.266\,900 \times 10^{-8}$	$0.608\,860 \times 10^{-17}$	$0.517\,962 \times 10^{-4}$	$0.778\,638 \times 10^{-6}$	$-0.217\,243 \times 10^{-15}$
1	$0.168\,162 \times 10^{-14}$	$0.461\,560 \times 10^{-22}$	$-0.112\,149 \times 10^{-7}$	$0.446\,396 \times 10^{-12}$	$0.104\,747 \times 10^{-20}$
2	$0.353\,075 \times 10^{-17}$	$0.184\,282 \times 10^{-24}$	$0.776\,507 \times 10^{-11}$	$0.784\,600 \times 10^{-15}$	$-0.523\,689 \times 10^{-23}$
3	$-0.963\,455 \times 10^{-20}$	$-0.524\,471 \times 10^{-27}$	$0.172\,569 \times 10^{-13}$	$-0.195\,151 \times 10^{-17}$	$0.817\,386 \times 10^{-26}$
4	$-0.223\,079 \times 10^{-22}$	$-0.121\,299 \times 10^{-29}$	$-0.320\,582 \times 10^{-16}$	$-0.542\,083 \times 10^{-20}$	$0.309\,913 \times 10^{-28}$
5	$0.453\,166 \times 10^{-25}$	$0.246\,512 \times 10^{-32}$	$-0.899\,435 \times 10^{-19}$	$0.103\,530 \times 10^{-22}$	$-0.363\,491 \times 10^{-31}$

Table 3. Fitting coefficients for the multivariate Taylor expansion (6) to the real part of the index of refraction over the $4.35 \leqslant 1/\sigma \leqslant 5.2$ μm range with $\sigma_{\rm ref} = 10^4/4.8$cm^{-1}.

j	$c_{j\rm ref}$ (cm^j)	c_{jT} (cm^j K)	c_{jTT} (cm^j K^2)	c_{jH} (cm^j %$^{-1}$)	c_{jHH} (cm^j %$^{-2}$)
0	$0.200\,020 \times 10^{-3}$	$0.590\,035 \times 10^{-1}$	$-4.098\,30$	$-0.140\,463 \times 10^{-7}$	$0.543\,605 \times 10^{-12}$
1	$0.275\,346 \times 10^{-9}$	$-0.375\,764 \times 10^{-6}$	$0.250\,037 \times 10^{-2}$	$0.839\,350 \times 10^{-11}$	$0.112\,802 \times 10^{-15}$
2	$0.325\,702 \times 10^{-12}$	$0.134\,585 \times 10^{-9}$	$0.275\,187 \times 10^{-6}$	$-0.190\,929 \times 10^{-14}$	$-0.229\,979 \times 10^{-19}$
3	$-0.693\,603 \times 10^{-14}$	$0.124\,316 \times 10^{-11}$	$-0.653\,398 \times 10^{-8}$	$-0.121\,399 \times 10^{-16}$	$-0.191\,450 \times 10^{-21}$
4	$0.285\,610 \times 10^{-17}$	$0.508\,510 \times 10^{-13}$	$-0.310\,589 \times 10^{-9}$	$-0.898\,863 \times 10^{-18}$	$-0.120\,352 \times 10^{-22}$
5	$0.338\,758 \times 10^{-18}$	$-0.189\,245 \times 10^{-15}$	$0.127\,747 \times 10^{-11}$	$0.364\,662 \times 10^{-20}$	$0.500\,955 \times 10^{-25}$
j	c_{jp} (cm^j Pa^{-1})	c_{jpp} (cm^j Pa^{-2})	c_{jTH} (cm^j K %$^{-1}$)	c_{jTp} (cm^{j}K Pa^{-1})	c_{jHp} (cm^j %$^{-1}$ Pa^{-1})
0	$0.266\,898 \times 10^{-8}$	$0.610\,706 \times 10^{-17}$	$0.674\,488 \times 10^{-4}$	$0.778\,627 \times 10^{-6}$	$-0.211\,676 \times 10^{-15}$
1	$0.273\,629 \times 10^{-14}$	$0.116\,620 \times 10^{-21}$	$-0.406\,775 \times 10^{-7}$	$0.593\,296 \times 10^{-12}$	$0.487\,921 \times 10^{-20}$
2	$0.463\,466 \times 10^{-17}$	$0.244\,736 \times 10^{-24}$	$0.289\,063 \times 10^{-11}$	$0.145\,042 \times 10^{-14}$	$-0.682\,545 \times 10^{-23}$
3	$-0.916\,894 \times 10^{-19}$	$-0.497\,682 \times 10^{-26}$	$0.819\,898 \times 10^{-13}$	$0.489\,815 \times 10^{-17}$	$0.942\,802 \times 10^{-25}$
4	$0.136\,685 \times 10^{-21}$	$0.742\,024 \times 10^{-29}$	$0.468\,386 \times 10^{-14}$	$0.327\,941 \times 10^{-19}$	$-0.946\,422 \times 10^{-27}$
5	$0.413\,687 \times 10^{-23}$	$0.224\,625 \times 10^{-30}$	$-0.191\,182 \times 10^{-16}$	$0.128\,020 \times 10^{-21}$	$-0.153\,682 \times 10^{-29}$

between 0 and 100 with a reference value set at $H_{\rm ref} = 10\%$ and σ the wavenumber $1/\lambda$ with a reference value set at $\sigma_{\rm ref}$. The units of these reference values match those of the tabulated coefficients. The range 1.3–2.5 μm is covered by table 1, the range 2.8–4.2 μm by table 2, the range 4.35–5.2 μm by table 3, the range 7.5–14.1 μm by table 4 and the range 16–24 μm by table 5.

Already in the Q band and then at sub-millimetre wavelengths and eventually in the static limit, the refractive index plotted as a function of wavelength is more and more structured by individual lines. Since we will not present these functions at high resolution but smooth fits within several bands in the infrared, their spiky appearance sets a natural limit to the far-IR wavelength regions that our approach may cover.

Table 4. Fitting coefficients for the multivariate Taylor expansion (6) to the real part of the index of refraction over the $7.5 \leqslant 1/\sigma \leqslant 14.1\ \mu$m range with $\sigma_{\mathrm{ref}} = 10^4/10.1\ \mathrm{cm}^{-1}$.

j	$c_{j\mathrm{ref}}$ (cm^j)	c_{jT} (cm^j K)	c_{jTT} (cm^j K^2)	c_{jH} (cm^j $\%^{-1}$)	c_{jHH} (cm^j $\%^{-2}$)
0	$0.199\,885 \times 10^{-3}$	$0.593\,900 \times 10^{-1}$	$-6.503\,55$	$-0.221\,938 \times 10^{-7}$	$0.393\,524 \times 10^{-12}$
1	$0.344\,739 \times 10^{-9}$	$-0.172\,226 \times 10^{-5}$	$0.103\,830 \times 10^{-1}$	$0.347\,377 \times 10^{-10}$	$0.464\,083 \times 10^{-15}$
2	$-0.273\,714 \times 10^{-12}$	$0.237\,654 \times 10^{-8}$	$-0.139\,464 \times 10^{-4}$	$-0.465\,991 \times 10^{-13}$	$-0.621\,764 \times 10^{-18}$
3	$0.393\,383 \times 10^{-15}$	$-0.381\,812 \times 10^{-11}$	$0.220\,077 \times 10^{-7}$	$0.735\,848 \times 10^{-16}$	$0.981\,126 \times 10^{-21}$
4	$-0.569\,488 \times 10^{-17}$	$0.305\,050 \times 10^{-14}$	$-0.272\,412 \times 10^{-10}$	$-0.897\,119 \times 10^{-19}$	$-0.121\,384 \times 10^{-23}$
5	$0.164\,556 \times 10^{-19}$	$-0.157\,464 \times 10^{-16}$	$0.126\,364 \times 10^{-12}$	$0.380\,817 \times 10^{-21}$	$0.515\,111 \times 10^{-26}$
j	c_{jp} (cm^j Pa^{-1})	c_{jpp} (cm^j Pa^{-2})	c_{jTH} (cm^j K $\%^{-1}$)	c_{jTp} ($\mathrm{cm}^j\mathrm{K}$ Pa^{-1})	c_{jHp} (cm^j $\%^{-1}$ Pa^{-1})
0	$0.266\,809 \times 10^{-8}$	$0.610\,508 \times 10^{-17}$	$0.106\,776 \times 10^{-3}$	$0.778\,368 \times 10^{-6}$	$-0.206\,365 \times 10^{-15}$
1	$0.695\,247 \times 10^{-15}$	$0.227\,694 \times 10^{-22}$	$-0.168\,516 \times 10^{-6}$	$0.216\,404 \times 10^{-12}$	$0.300\,234 \times 10^{-19}$
2	$0.159\,070 \times 10^{-17}$	$0.786\,323 \times 10^{-25}$	$0.226\,201 \times 10^{-9}$	$0.581\,805 \times 10^{-15}$	$-0.426\,519 \times 10^{-22}$
3	$-0.303\,451 \times 10^{-20}$	$-0.174\,448 \times 10^{-27}$	$-0.356\,457 \times 10^{-12}$	$-0.189\,618 \times 10^{-17}$	$0.684\,306 \times 10^{-25}$
4	$-0.661\,489 \times 10^{-22}$	$-0.359\,791 \times 10^{-29}$	$0.437\,980 \times 10^{-15}$	$-0.198\,869 \times 10^{-19}$	$-0.467\,320 \times 10^{-29}$
5	$0.178\,226 \times 10^{-24}$	$0.978\,307 \times 10^{-32}$	$-0.194\,545 \times 10^{-17}$	$0.589\,381 \times 10^{-22}$	$0.126\,117 \times 10^{-30}$

Table 5. Fitting coefficients for the multivariate Taylor expansion (6) to the real part of the index of refraction over the $16 \leqslant 1/\sigma \leqslant 24\ \mu$m range with $\sigma_{\mathrm{ref}} = 10^4/20\ \mathrm{cm}^{-1}$.

j	$c_{j\mathrm{ref}}$ (cm^j)	c_{jT} (cm^j K)	c_{jTT} (cm^j K^2)	c_{jH} (cm^j $\%^{-1}$)	c_{jHH} (cm^j $\%^{-2}$)
0	$0.199\,436 \times 10^{-3}$	$0.621\,723 \times 10^{-1}$	$-23.240\,9$	$-0.772\,707 \times 10^{-7}$	$-0.326\,604 \times 10^{-12}$
1	$0.299\,123 \times 10^{-8}$	$-0.177\,074 \times 10^{-4}$	$0.108\,557$	$0.347\,237 \times 10^{-9}$	$0.463\,606 \times 10^{-14}$
2	$-0.214\,862 \times 10^{-10}$	$0.152\,213 \times 10^{-6}$	$-0.102\,439 \times 10^{-2}$	$-0.272\,675 \times 10^{-11}$	$-0.364\,272 \times 10^{-16}$
3	$0.143\,338 \times 10^{-12}$	$-0.954\,584 \times 10^{-9}$	$0.634\,072 \times 10^{-5}$	$0.170\,858 \times 10^{-13}$	$0.228\,756 \times 10^{-18}$
4	$0.122\,398 \times 10^{-14}$	$-0.996\,706 \times 10^{-11}$	$0.762\,517 \times 10^{-7}$	$0.156\,889 \times 10^{-15}$	$0.209\,502 \times 10^{-20}$
5	$-0.114\,628 \times 10^{-16}$	$0.921\,476 \times 10^{-13}$	$-0.675\,587 \times 10^{-9}$	$-0.150\,004 \times 10^{-17}$	$-0.200\,547 \times 10^{-22}$
j	c_{jp} (cm^j Pa^{-1})	c_{jpp} (cm^j Pa^{-2})	c_{jTH} (cm^j K $\%^{-1}$)	c_{jTp} ($\mathrm{cm}^j\mathrm{K}$ Pa^{-1})	c_{jHp} (cm^j $\%^{-1}$ Pa^{-1})
0	$0.266\,827 \times 10^{-8}$	$0.613\,675 \times 10^{-17}$	$0.375\,974 \times 10^{-3}$	$0.778\,436 \times 10^{-6}$	$-0.272\,614 \times 10^{-15}$
1	$0.120\,788 \times 10^{-14}$	$0.585\,494 \times 10^{-22}$	$-0.171\,849 \times 10^{-5}$	$0.461\,840 \times 10^{-12}$	$0.304\,662 \times 10^{-18}$
2	$0.522\,646 \times 10^{-17}$	$0.286\,055 \times 10^{-24}$	$0.146\,704 \times 10^{-7}$	$0.306\,229 \times 10^{-14}$	$-0.239\,590 \times 10^{-20}$
3	$0.783\,027 \times 10^{-19}$	$0.425\,193 \times 10^{-26}$	$-0.917\,231 \times 10^{-10}$	$-0.623\,183 \times 10^{-16}$	$0.149\,285 \times 10^{-22}$
4	$0.753\,235 \times 10^{-21}$	$0.413\,455 \times 10^{-28}$	$-0.955\,922 \times 10^{-12}$	$-0.161\,119 \times 10^{-18}$	$0.136\,086 \times 10^{-24}$
5	$-0.228\,819 \times 10^{-24}$	$-0.812\,941 \times 10^{-32}$	$0.880\,502 \times 10^{-14}$	$0.800\,756 \times 10^{-20}$	$-0.130\,999 \times 10^{-26}$

The calculation adopts a standard of 370 ppmv of CO_2 as the most likely contemporary ambient clean air standard [64–66], well aware that laboratory air may contain a higher volume fraction. Although adding this mixing ratio as another free parameter to the procedure is feasible, it has been kept fixed here to keep the size of the tables in check.

Solely for the benefit of the reader who may use this type of result as a black box, the parameter set in (6) is based on relative humidity rather than some more fundamental measure of the water molecule number density; the more appealing alternative from a scholarly point of view would have been to split the computational steps into

(i) equations to calculate absolute molecular number densities, plus

(ii) the fitting equations to transform these to polarizabilities, and

(iii) some post-processing with (4).

The first step involves a self-consistent adaptation of the components of the dry air at given mixing ratios to a partial pressure that is 'left over' from p after settling for the water density. The philosophy behind equation (6) is to take this kind of burden away.

The negative values of c_{0H} paraphrase that substitution of the 'average' dry air molecule by water at a fixed total pressure p decreases the refractive index in all our wavelength regions.

The well-known disadvantage inherent to the polynomial ansatz (5) σ, is the appearance of artificial wiggles as a function of σ, the number of which is set by the maximum power of j. At any fixed triple (T, p, H), one may in fact fit the raw data better if (5) is replaced by a Sellmeier format with two resonances [67]. An attempt to expand each of the five free parameters of this alternative representation in the style of (6) did not achieve competitive stability over the same range of temperature, pressure and humidity, so this route is not documented here.

4. Comparison with experiments

The raw theoretical data—prior to the fit—exceed experiments for dry air in the visible and near-infrared by $\approx 4 \times 10^{-8}$ (figure 1). Approximately 0.8×10^{-8} of this can be attributed to a change in temperature scales [68], and approximately 1×10^{-8} to a presumably lower CO_2 content of 300 ppmv in [15].

The pressure coefficient c_{0p} for dry air at 10 μm in table 4 is to be compared to the value of 2.668×10^{-4} $\mathrm{atm}^{-1} = 0.2633 \times 10^{-8}$ Pa^{-1} measured by Marchetti and Simili [20,

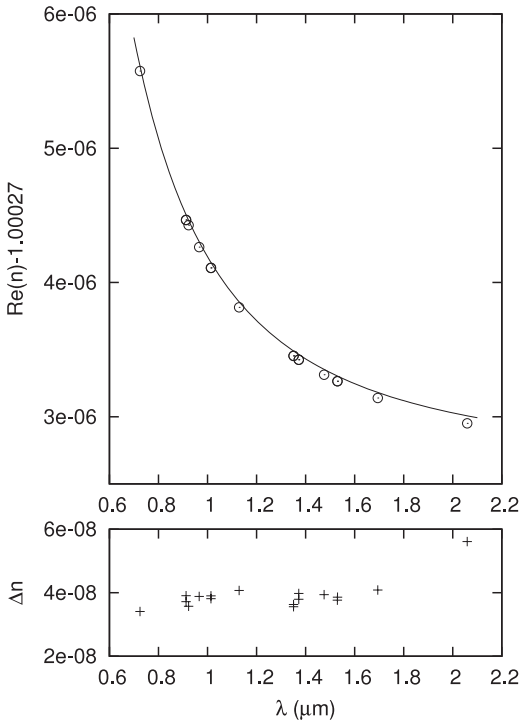

Figure 1. Top: the line is the raw data of the theory for dry air at 15 °C and 1013.24 hPa. Circles are the experimental values of tables 1 and 2 by Peck and Reeder [15] plus one datum at 2.06 μm by Peck and Khanna [14]. Bottom: refractive index of the theory minus these experimental values.

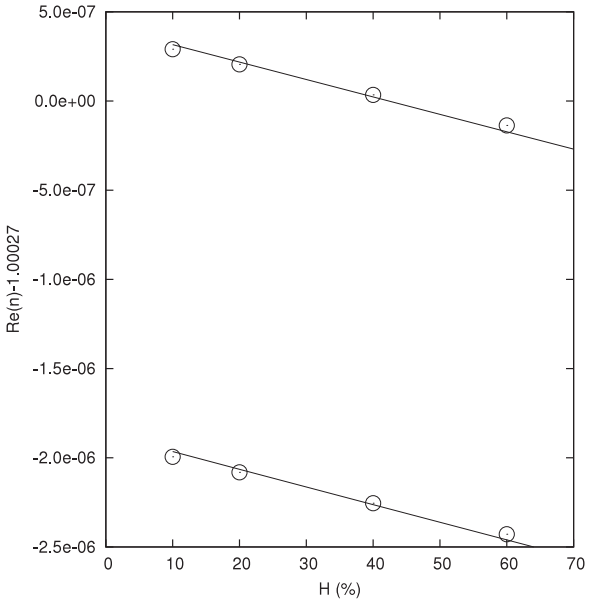

Figure 2. Lines are the raw data of the theory for humid air at 20 °C and 1000 hPa at four levels of humidity. Circles are from the Bönsch–Potulski fitting equation (at 370 ppm CO_2) to their experimental data [2]. The upper group refers to $\lambda = 0.5087$ μm, the lower to $\lambda = 0.644$ μm.

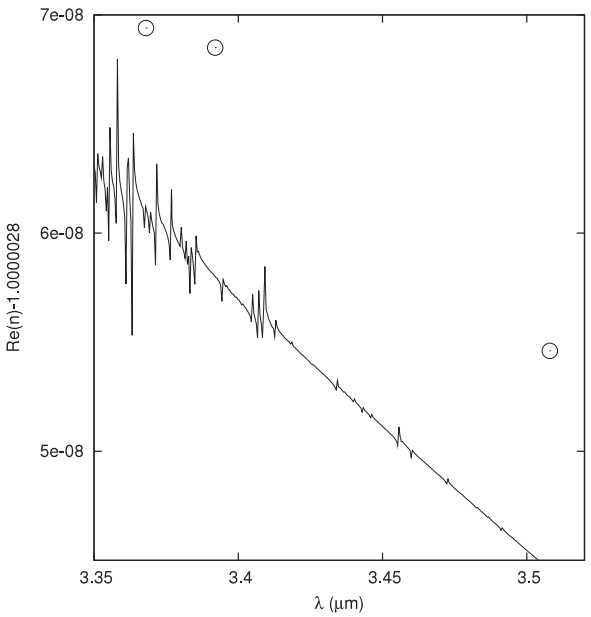

Figure 3. Comparison of the theory (solid line) with the experimental data by Matsumoto (3 circles) [5, table 1] for water vapour of 1333 Pa at 20 °C.

table 1][1] at $\lambda = 10.57$ μm and $T = 23$ °C. More accurately, the pressure gradient predicted from (6) is

$$\frac{\partial n}{\partial p} = \sum_{j=0,1,\ldots} \left[c_{jp} + 2c_{jpp}\,(p - p_{\mathrm{ref}}) + c_{jTp}\left(\frac{1}{T} - \frac{1}{T_{\mathrm{ref}}}\right) + c_{jHp}\,(H - H_{\mathrm{ref}}) \right] (\sigma - \sigma_{\mathrm{ref}})^j \qquad (7)$$

and generates 0.2618×10^{-8} Pa^{-1} at the same wavelength, the same temperature and a pressure—not documented by Marchetti and Simili—of 1013.25 hPa. The relative deviation of 6×10^{-3} between experiment and theory is still compatible with the error 5×10^{-3} provided by Marchetti and Simili.

The theory deviates from the humid air data at the longest two wavelengths of the Bönsch–Potulski experiments [2] by 3.5×10^{-8} or less: figure 2.

The difference between the theory and experiments with pure water vapour (figure 3) and moist air (figure 4) is $\approx 1 \times 10^{-8}$ at 3.4 μm.[2] In these two figures, two or four of the most significant digits of the susceptibility have been artificially suppressed—note the labels on the ordinate axes. Therefore, the difference between theory and experiment measured as the relative deviation between the susceptibilities may appear large at first glance, but it is only 3×10^{-3} in figure 3 and 3×10^{-5} in figure 4. The two figures are drawn at large zoom factors to illustrate that the amplitudes caused by individual transitions start to be of comparable magnitude at this level of precision [69].

At this point, we explicitly avoid contact with the secondary literature that was placed in a 'review' category in the first section. It is tempting to extrapolate a few-parameter fits from the visible into the IR, but there they (as my parametrization here) remain essentially unchallenged and unsupported by experimental evidence.

[1] Presumably, the factor 10^{-4} ought to be 10^{+4} and the 296 °C to be 23 °C in their table 1.

[2] In table 2 of [5], we assume that the f value is 1333, not 133 Pa, and that the three values refer to the three different wavelengths of table 1, not to two wavelengths.

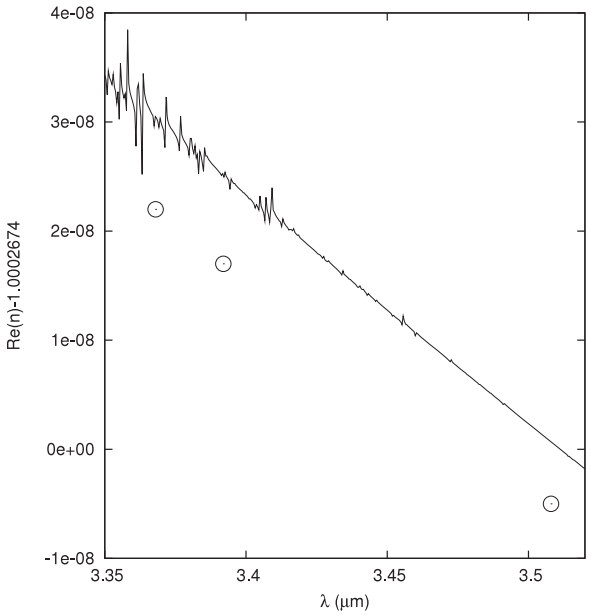

Figure 4. Comparison of the theory (solid line, 300 ppmv CO_2) with the experimental data by Matsumoto (3 circles) [5, table 2] for humid air at $p = 1013.25$ hPa, $T = 20\,^{\circ}$C and $H = 56.98\%$.

The error propagation for any application is simple, because χ is almost proportional to the molecular densities. If the contribution of the water vapour to the refractive index is $\chi \approx 3\times10^{-6}$ as in figure 3, for example, one would start to ask for a computational formalism more accurate than $\approx 3 \times 10^{-8}$ if one could supply this humidity with a relative error less than 1×10^{-2}.

5. Summary

A theory of refractive index calculations for modestly humid air at fixed 370 parts-per-million volume fraction of carbon dioxide has been condensed into simple fits. The parameter range covers infrared wavelengths from 1.3 to 24 μm, and the common ambient air pressures and temperatures at sites of ground-based telescopes. The need for such a theoretical approach arises from lack of experimental data for wavelengths above 1.7 μm, and from the complexity of the electromagnetic dispersion which invalidates formulae which extrapolate from air dispersion in the visible.

The inherent accuracy of the Taylor series representation has been aligned with the estimated accuracy of the underlying theory. In consequence, the eventual accuracy of any real-world application is more likely to be limited by the errors in the input parameters (that is, in particular, the knowledge of the humidity of an air sample) than by the residuals of the fitting approach.

Acknowledgment

This work is supported by the NWO VICI grant 2010010237.

References

[1] Barrell H and Sears J E 1939 *Phil. Trans. R. Soc.* A **238** 1–64
[2] Bönsch G and Potulski E 1998 *Metrologia* **35** 133–9
[3] Newbound K B 1949 *J. Opt. Soc. Am.* **39** 835–40
[4] Cuthbertson C and Cuthbertson M 1913 *Phil. Trans. R. Soc.* A **213** 1–26
[5] Matsumoto H 1982 *Metrologia* **18** 49–52
[6] Matsumoto H 1984 *Opt. Commun.* **50** 356–8
[7] Marchetti S and Simili R 2006 *Infrared Phys. Technol.* **48** 115–21
[8] Birch K P 1991 *J. Opt. Soc. Am.* A **8** 647–51
[9] Hou W and Thalmann R 1994 *Measurement* **13** 307–14
[10] Edlén B 1953 *J. Opt. Soc. Am.* **43** 339–44
[11] Zhang J, Lu Z H and Wang L J 2005 *Opt. Lett.* **30** 3314–6
[12] Velsko S P and Eimerl D 1986 *Appl. Opt.* **25** 1344–9
[13] Peck E R 1986 *Appl. Opt.* **25** 3597–8
[14] Peck E R and Khanna B N 1962 *J. Opt. Soc. Am.* **52** 416–9
[15] Peck E R and Reeder K 1972 *J. Opt. Soc. Am.* **62** 958–62
[16] Old J G, Gentili K L and Peck E R 1971 *J. Opt. Soc. Am.* **61** 89–90
[17] Jhanwar B L and Meath W J 1982 *Chem. Phys.* **67** 185–99
[18] Rank D H, Saksena G D and McCubbin T K Jr 1958 *J. Opt. Soc. Am.* **48** 455–8
[19] Simmons A C 1978 *Opt. Commun.* **25** 211–4
[20] Marchetti S and Simili R 2006 *Infrared Phys. Technol.* **47** 263–6
[21] Tubbs R N, Meisner J A, Bakker E J and Albrecht S 2004 Astronomical telescopes and instrumentation *Proc. SPIE* **5491** 588–99
[22] Schiebener P, Straub J, Levelt Sengers J M H and Gallagher J S 1990 *J. Phys. Chem. Ref. Data* **19** 677–717
[23] Ciddor P E 1996 *Appl. Opt.* **35** 1566–73
[24] Owens J C 1967 *Appl. Opt.* **6** 51–9
[25] Jones F E 1980 *Appl. Opt.* **19** 4129–30
[26] Harvey A H, Gallagher J S and Levelt Sengers J M H 1998 *J. Phys. Chem. Ref. Data* **27** 761–74
[27] Colavita M M, Swain M R, Akeson R L, Koresko C D and Hill R J 2004 *Publ. Astron. Soc. Pac.* **116** 876–85
[28] Mathar R J 2004 *Appl. Opt.* **43** 928–32
[29] Hill R J and Lawrence R S 1986 *Infrared Phys.* **26** 371–6
[30] Hill R J, Clifford S F and Lawrence R S 1980 *J. Opt. Soc. Am.* **70** 1192–205
[31] Basden A G and Buscher D F 2005 *Mon. Not. R. Astron. Soc.* **357** 656–68
[32] Mathar R J 2006 *Preprint* astro-ph/0605304
[33] Meisner J A and Le Poole R S 2003 Interferometry for optical astronomy II *Proc. SPIE* **4838** 609–24
[34] Berton R P H 2006 *J. Opt. A: Pure Appl. Opt.* **8** 817–30
[35] Rothman L S *et al* 2005 *J. Quant. Spectrosc. Radiat. Transfer* **96** 139–204
[36] Hilborn R C 1981 *Am. J. Phys.* **50** 982–6
[37] Smith K M, Ptashnik I, Newnham D A and Shine K P 2004 *J. Quant. Spectrosc. Radiat. Transfer* **83** 735–49
[38] Tanaka T, Fukabori M, Sugita T, Nakajima H, Yokota T, Watanabe T and Sasano Y 2006 *J. Mol. Spectrosc.* **239** 1–10
[39] Dymond J H and Smith E B 1980 *The Virial Coefficients of Pure Gases and Mixtures* (Oxford: Clarendon)
[40] Weber L A 1970 *J. Res. Nat. Bur. Stand.* A **74** 93–129
[41] Lemmon E W, Jacobsen R T, Penoncello S G and Friend D G 2000 *J. Phys. Chem. Ref. Data* **29** 331–85
[42] Achtermann H J, Magnus G and Bose T K 1991 *J. Chem. Phys.* **94** 5669–84
[43] Kell G S, McLaurin G E and Whalley E 1989 *Proc. R. Soc.* A **425** 49–71
[44] Kusalik P G, Liden F and Svishchev I M 1995 *J. Chem. Phys.* **103** 10169–75
[45] Hill P G and MacMillan R D C 1988 *Ind. Eng. Chem. Res.* **27** 874–82
[46] Wagner W and Pruß A 2002 *J. Phys. Chem. Ref. Data* **31** 387–535
[47] Sato H, Watanabe K, Levelt Sengers J M H, Gallagher J S, Hill P G, Straub J and Wagner W 1991 *J. Phys. Chem. Ref. Data* **20** 1023–44
[48] Harvey A H and Lemmon E W 2004 *J. Phys. Chem. Ref. Data* **33** 369–76

[49] Natl Inst. Stand. Technol. 2006 Database of the thermodynamical properties of gases used in semiconductor industry *Tech. Rep.* 134 NIST
[50] Barber R J, Tennyson J, Harris G J and Tolchenov R N 2006 *Mon. Not. R. Astron. Soc.* **368** 1087–94
[51] Šimečková M, Jacquemart D, Rothman L S, Gamache R R and Goldman A 2006 *J. Quant. Spectrosc. Radiat. Transfer* **98** 130–55
[52] Gamache R R, Kennedy S, Hawkins R and Rothman L S 2000 *J. Mol. Struct.* **517/518** 407–25
[53] Toth R A, Brown L R, Smith M A H, Malathy Devi V, Benner D C and Dulick M 2005 *J. Quant. Spectrosc. Radiat. Transfer* **101** 339–66
[54] Jacquemart D, Gamache R and Rothman L S 2005 *J. Quant. Spectrosc. Radiat. Transfer* **96** 205–39
[55] Slanina Z, Uhlík F, Lee S L and Nagase S 2006 *J. Quant. Spectrosc. Radiat. Transfer* **97** 415–23
[56] Havens G G 1933 *Phys. Rev.* **43** 992–1000
[57] Davis R S 1998 *Metrologia* **35** 49–55
[58] Boreiko R T, Smithson T L, Clark T A and Wieser H 1984 *J. Quant. Spectrosc. Radiat. Transfer* **32** 109–17
[59] Krupenie P H 1972 *J. Phys. Chem. Ref. Data* **1** 423–534
[60] Chance K V, Traub W A, Jucks K W and Johnson D G 1991 *Int. J. Infrared Millim. Waves* **12** 581–8
[61] Cini R and Torrini M 1968 *J. Chem. Phys.* **49** 2826–30
[62] de Wolf D A 1993 *J. Opt. Soc. Am.* A **10** 1544–8
[63] de Goede J and Mazur P 1972 *Physica* **58** 568–84
[64] Cooperative Atmospheric Data Integration Project 2003 GLOBALVIEW-CO_2 *Tech. Rep.* NOAA/CMDL ftp://ftp.cmdl.noaa.gov/ccg/co2/GLOBALVIEW
[65] Yang Z, Toon G C, Margolis J S and Wennberg P O 2002 *Geophys. Res. Lett.* **29** 53–4
[66] Kane R P and de Paula E R 1996 *J. Atmos. Terr. Phys.* **58** 1673–81
[67] Peck E R 1983 *Appl. Opt.* **22** 2906–13
[68] Birch K P and Downs M J 1993 *Metrologia* **30** 155–62
[69] Galkin Y S and Tatevian R A 1991 *J. Geod.* **71** 680–4